Chapter 12
Longitudinal Wave Propagation Including High Frequency Component in Viscoelastic Bars

T. Tamaogi and Y. Sogabe

Abstract The purpose of this study to evaluate the attenuation and the dispersion properties for viscoelastic materials over a wide range of frequencies. The viscoelastic properties within the frequency of around 200 kHz were examined by using the solid and hollow bars of polymethyl methacrylate (PMMA). The PMMA properties were testes by the longitudinal impact experiments in the lower frequency area of up to around 15 kHz and the ultrasonic propagation experiments using the ultrasonic transducers in the high frequency area from 20 to 200 kHz. Consequently, it was found that the second-mode vibration as well as the first-mode should be considered in the high frequency area. It was also confirmed that the second-mode vibration influenced deeply as the radial thickness became thin.

Keywords Dynamic properties • Propagation • Viscoelastic • Ultrasonic • Transducer

12.1 Introduction

Polymer materials are widely used in various fields because of their impact resistance or the vibration control. It is well known that the deformation of the materials remarkably depends on the time or the strain rate. The shape of a stress wave in a viscoelastic bar changes as it propagates because of the attenuation and the dispersion that mainly depend on the material damping characteristics. The dynamic properties of viscoelastic materials have been evaluated by some techniques such as the wave propagation method [1, 2] and the viscoelastic SHB method [3, 4] based on the elementary theory. Taking the geometric dispersion or the three-dimensional effect into account, more precise theories have been demonstrated [5, 6].

The dynamic properties of viscoelastic materials in the high frequency area are complex, but it is difficult to evaluate the properties only by the impact experiment. In this work, the ultrasonic propagation experiments as well as the longitudinal impact experiments were performed using PMMA materials in order to evaluate the attenuative and dispersive features over a wide range of frequencies based on the three-dimensional exact theory.

12.2 Viscoelastic Theory

12.2.1 Viscoelastic Model

In the case of a thin and uniform viscoelastic bar, the constitutive equation about for a one-dimensional longitudinal wave is written in the following form:

$$P(D)\sigma(x,t) = Q(D)\varepsilon(x,t), \tag{12.1}$$

where x is the coordinate along the rod axis, t is the time, ρ is the material density, σ and ε are stress and strain along the x-axis, respectively. D denotes the differentiation with respect to time $D=\partial/\partial t$, $p(D)$ and $Q(D)$ are linear differentiation operators.

T. Tamaogi (✉)
Department of Mechanical Engineering, National Institute of Technology, Niihama College, 7-1 Yakumo-cho, Niihama, Ehime 792-8580, Japan
e-mail: takatamajp@yahoo.co.jp

Y. Sogabe
Department of Mechanical Engineering, Ehime University, 3 Bunkyo-cho, Matsuyama, Ehime 790-8577, Japan

B. Song et al. (eds.), *Dynamic Behavior of Materials, Volume 1*,
Conference Proceedings of the Society for Experimental Mechanics Series, DOI 10.1007/978-3-319-22452-7_12

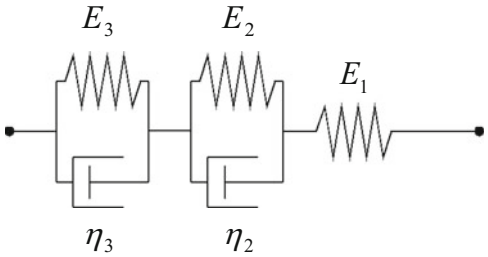

Fig. 12.1 Viscoelastic models for determining mechanical properties

The complex compliance, which represents one of the viscoelastic properties of the material, is defined by the ratio of strain to stress in the frequency domain as

$$J^*(\omega) = {J_1}^*(\omega) - i\ {J_2}^*(\omega). \tag{12.2}$$

The viscoelastic characteristics of materials are identified as 5-element model in this paper as shown in Fig. 12.1. The relation between viscoelastic parameters of 5-element model and the real and the imaginary part of the complex compliance are given by

$$\left.\begin{aligned} {J_1}^*(\omega) &= \frac{1}{E_1} + \frac{E_2}{{E_2}^2 + (\omega\eta_2)^2} \\ {J_2}^*(\omega) &= \frac{\omega\eta_2}{{E_2}^2 + (\omega\eta_2)^2} \end{aligned}\right\}. \tag{12.3}$$

The Poisson's ratio of a viscoelastic medium ν can be assumed to be a real constant as well as the elastic medium. The complex Lame's functions $\lambda^*(\omega)$ and $\mu^*(\omega)$ are shown as follows by using ν and $J^*(\omega)$:

$$\left.\begin{aligned} \lambda^*(\omega) &= \frac{\nu}{(1+\nu)(1-2\nu)J^*(\omega)} \\ \mu^*(\omega) &= \frac{1}{2(1+\nu)J^*(\omega)} \end{aligned}\right\}. \tag{12.4}$$

12.2.2 Three-Dimensional Exact Theory

Consider a stress wave propagating in an infinite cylindrical elastic bar. The equation of motion is written in the following

$$\rho\frac{\partial^2 \mathbf{u}}{\partial t^2} = (\lambda + 2\mu)\mathrm{grad}\Delta - 2\mu\mathrm{rot}\ \boldsymbol{\Omega}, \tag{12.5}$$

where $\mathbf{u}$ denotes the displacement vector, λ and μ are the Lame coefficients, Δ=div$\boldsymbol{u}$, $2\boldsymbol{\Omega}$=rot$\boldsymbol{u}$. Assuming axial symmetry, and applying the Fourier transformation with respect to the time and the correspondence principle [7] to (12.5), the following equations for a viscoelastic medium on the cylindrical coordinate plane are deduced:

$$\left.\begin{aligned} -\rho\omega^2 U_r &= \left(\lambda^* + 2\mu^*\right)\frac{\partial D}{\partial r} - 2i\xi\mu^* W \\ -\rho\omega^2 U_z &= \left(\lambda^* + 2\mu^*\right)(-i\xi)D - 2\mu^*\left(\frac{\partial W}{\partial r} + \frac{W}{r}\right) \end{aligned}\right\}, \tag{12.6}$$

where the displacement $\overline{u}_r(r,z,\omega)$=$U_r(r,\omega)\cdot\exp(-i\xi z)$ and $\overline{u}_z(r,z,\omega)$=$U_z(r,\omega)\cdot\exp(-i\xi z)$, the volumetric strain $\overline{\Delta}(r,z,\omega)$=$D(r,\omega)\cdot\exp(-i\xi z)$, the rotation vector $\overline{\Omega}_\theta(r,z,\omega)$=$W(r,\omega)\cdot\exp(-i\xi z)$, $\xi(\omega)$=$k(\omega) - i\alpha(\omega)$ respectively. Solving (12.7) in D and W of solid and hollow bars, the Bessel's differential equations are obtained. The solutions can be expressed as follows: The subscript s and h means solid and hollow bars, respectively.

$$\left.\begin{aligned} D_s(r,\omega) &= A_0 J_0(pr) \\ W_s(r,\omega) &= A_1 J_1(qr) \end{aligned}\right\}, \tag{12.7}$$

$$\left.\begin{aligned} D_h(r,\omega) &= A_0 J_0(pr) + B_0 Y_0(pr) \\ W_h(r,\omega) &= A_1 J_1(qr) + B_1 Y_1(qr) \end{aligned}\right\}, \tag{12.8}$$

where J_0, and J_1 are the Bessel functions of first kind, Y_0, and Y_1 are those of second kind. A_0, A_1, B_0 and B_1 are the arbitrary functions of ω, $p^2=\rho\omega^2/\left(\lambda^*+2\mu^*\right)-\xi^2$, $q^2=\rho\omega^2/\mu^*-\xi^2$, respectively. The displacement and Stress are calculated from above equations. Considering stress free boundary conditions at the external surface of the bar, the following frequency equation results of solid and hollow bars:

$$\begin{vmatrix} c_{11} & c_{12} \\ c_{21} & c_{22} \end{vmatrix} = 0, \tag{12.9}$$

$$\begin{vmatrix} c_{11} & c_{12} & c_{13} & c_{14} \\ c_{21} & c_{22} & c_{23} & c_{24} \\ c_{31} & c_{32} & c_{33} & c_{34} \\ c_{41} & c_{42} & c_{43} & c_{44} \end{vmatrix} = 0, \tag{12.10}$$

where $c_{11}=\left(q^2-\xi^2\right)J_0(pa)-2pJ_1(pa)/a$, $c_{12}=(2i\xi)[qJ_0(qa)-J_1(qa)/a]$, $c_{13}=\left(q^2-\xi^2\right)Y_0(pa)-2pY_1(pa)/a$, $c_{14}=(2i\xi)[qY_0(qa)-Y_1(qa)/a]$, $c_{21}=2i\xi pJ_1(pa)$, $c_{22}=\left(q^2-\xi^2\right)J_1(qa)$, $c_{23}=2i\xi pY_1(pa)$, $c_{24}=\left(q^2-\xi^2\right)Y_1(qa)$, $c_{31}=\left(q^2-\xi^2\right)J_0(pb)-2pJ_1(pb)/b$, $c_{32}=(2i\xi)[qJ_0(qb)-J_1(qb)/b]$, $c_{33}=\left(q^2-\xi^2\right)Y_0(pb)-2pY_1(pb)/b$, $c_{34}=(2i\xi)[qY_0(qb)-Y_1(qb)/b]$, $c_{41}=2i\xi pJ_1(pb)$, $c_{42}=\left(q^2-\xi^2\right)J_1(qb)$, $c_{43}=2i\xi pY_1(pb)$, $c_{44}=\left(q^2-\xi^2\right)Y_1(qb)$,

a and b are the outer and inner radii, respectively.

Solving (12.9) and (12.10) for complex wave number $\xi(\omega)$ numerically, the attenuation coefficient $\alpha(\omega)$, the wave number $k(\omega)$ and the phase velocity $C(\omega)$ are given by

$$\alpha(\omega) = -\mathrm{Im}[\xi(\omega)], \tag{12.11}$$

$$k(\omega) = \mathrm{Re}[\xi(\omega)], \tag{12.12}$$

$$C(\omega) = \frac{\omega}{k(\omega)}. \tag{12.13}$$

12.3 Experimental Methods

The longitudinal wave propagation experiments and the ultrasonic propagation experiments using the ultrasonic transducers were carried out. The experimental methods and dimensions using the PMMA solid bars were indicated in reference [8].

Figure 12.2 shows a schematic diagram of an ultrasonic wave propagation experiment using wave packets generated by the ultrasonic transducers when the PMMA hollow bars are used. The length and outer and inner diameter are 1000 mm, 15 mm and 9 mm, respectively. Six kinds of ultrasonic transducers having several characteristic frequencies from 20 to 200 kHz are prepared as shown in Table 12.1. The ultrasonic transducer is attached to the one side of the specimen. Four semiconductor strain gages are situated on the outer surface separated by equal intervals. The transducer is vibrated at the natural frequency by giving the voltage amplified with an AC amplifier.

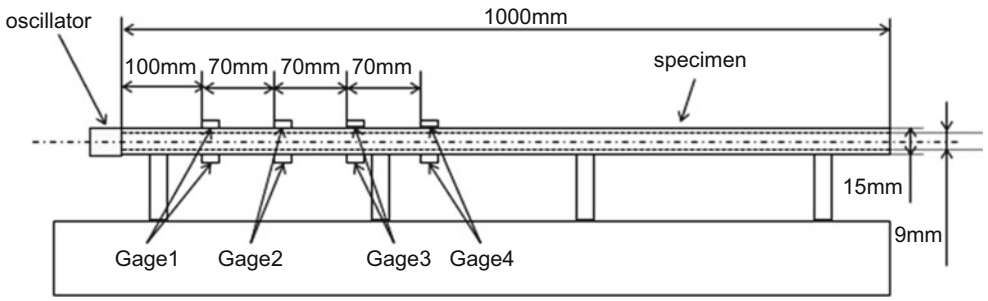

Fig. 12.2 Schematic diagram of propagation experiment using wave packets generated by ultrasonic transducer

Table 12.1 Properties of ultrasonic transducers (Fuji Ceramics Corporation)

Type		Frequency kHz	Diameter mm	Length mm	Capacitance pF
①	0.05Z15D	49.75	15	26.20	136
②	0.075Z15D	74.95	15	16.40	220
③	0.1Z15D	99.60	15	10.50	339
④	0.13Z10D	131.40	10	8.40	192
⑤	0.15Z20D	148.50	20	8.40	788
⑥	0.2Z15D	198.70	15	6.20	564

12.4 Experimental Results and Analyses

12.4.1 Measurement Results and Attenuative and Dispersive Features

The measured strain waves using the ultrasonic transducer type ① (49.75 kHz) on a PMMA hollow bar is denoted in Fig. 12.3a as a typical example. It is found that the attenuation and dispersion generate as the waves propagate. The frequency spectrum of each wave are represented in Fig. 12.3b. The frequency spectrums have a lot of frequency elements of in the frequency around 50 kHz. The values of 46.9–50.3 kHz, which are 70 % of the maximum values of the frequency spectrums, are used for evaluation of the attenuative and dispersive features.

The strain wave propagating on the surface of the bar is obtained by the following equation [8]:

$$\overline{\varepsilon}_z = \overline{\varepsilon}_0 \exp\{-(\alpha + ik)\}z, \tag{12.14}$$

where z is the coordinate along the rod axis, $\overline{\varepsilon}$ indicates the strain in the frequency domain. Using the least square method, the attenuation coefficient and phase velocity can be determined from the experimental data [8].

The attenuation coefficient and phase velocity on the hollow and solid bar (the diameter is 8 mm) are shown in Figs. 12.4 and 12.5. The plots in the figures show average experimental values, and the vertical bars indicate the standard deviation. The solid line is the analytical values obtained by the solution for the first mode of the complex wave number using 5-element model shown in Fig. 12.1. The viscoelastic values E_1, E_2, η_2, E_3 and η_3 are 5.89 GPa, 58.4 GPa, 2.80 MPa·s, 122 GPa, 0.39 MPa·s.

It is found that the experimental and model's predicted values for both $\alpha(\omega)$ and $C(\omega)$ on solid bar are almost identical in Fig. 12.5a, b. It is enough to evaluate the properties for the PMMA solid bar of a wide range of frequencies using the first mode of the complex wave number. In contrast, the experimental and model's predicted values for both $\alpha(\omega)$ and $C(\omega)$ on hollow coincide with each other within the low frequency area in Fig. 12.4a, b. However, experimental and analytical values are disagreement in the high frequency area. It is considered that the high-order mode vibrations are generated.

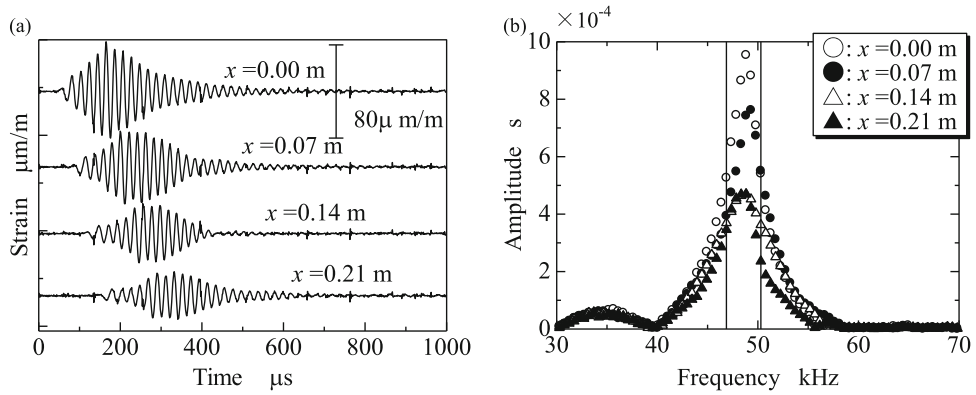

Fig. 12.3 Experimental results on propagation test using wave packets generated by ultrasonic transducer type ① (49.75 kHz) on PMMA hollow bar. (**a**) Measured strain waves; (**b**) frequency spectrums

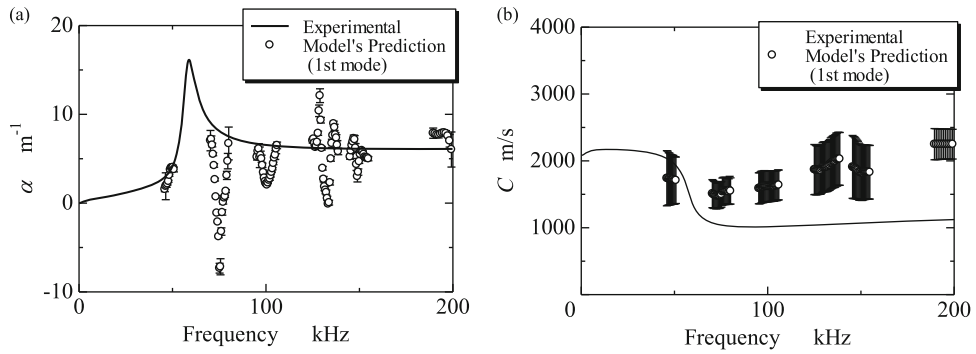

Fig. 12.4 Experimental and analytical values for $\alpha(\omega)$ and $C(\omega)$ on PMMA hollow bar. (**a**) Attenuation coefficient; (**b**) phase velocity

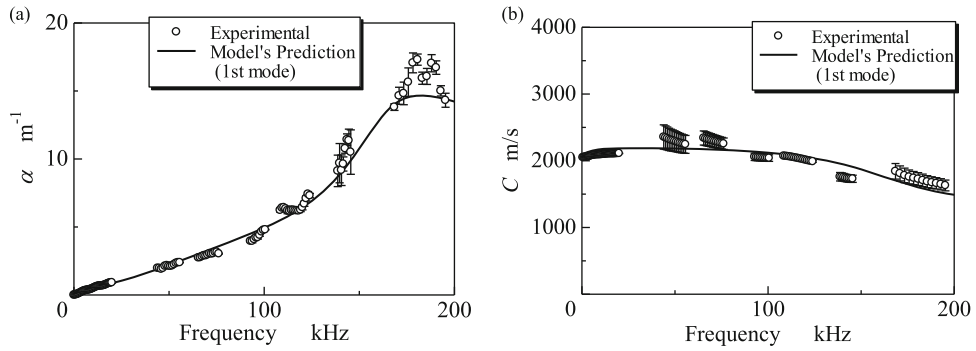

Fig. 12.5 Experimental and analytical values of $\alpha(\omega)$ and $C(\omega)$ on PMMA solid bar with diameter of 8 mm. (**a**) Attenuation coefficient; (**b**) phase velocity

12.4.2 Effect of High-Order Mode for Hollow Bar

Figure 12.6 shows the model's predicted values of first and second mode solutions for $\alpha(\omega)$ and $C(\omega)$ on the hollow bar with the outer and inner diameter of 15 and 9 mm. It is seen that the value of the second mode become small remarkably in the frequency around 65 kHz, and is almost the same value of the first mode. It is verified that the disagreement between the experimental and the analytical values in the high frequency area in Figs. 12.4a, b is due to the higher-order mode vibration. Therefore, it can be said that the higher-order mode vibration as well as the first mode vibration propagate on the hollow bar in the high frequency area.

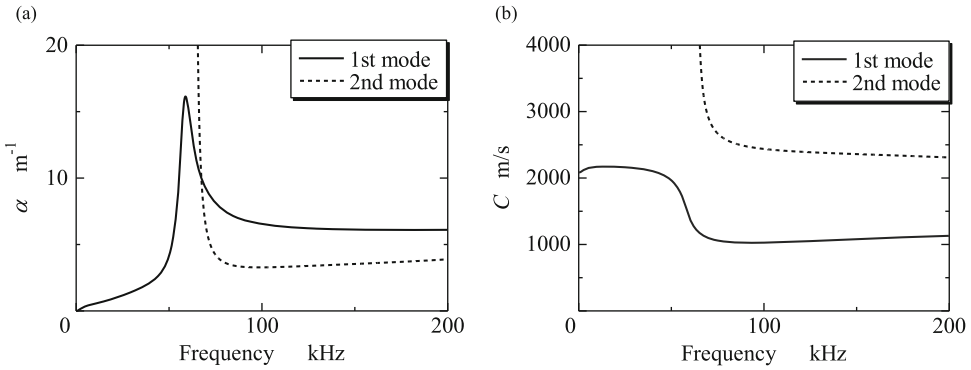

Fig. 12.6 Analytical values of first and second mode for $\alpha(\omega)$ and $C(\omega)$ on PMMA hollow bar. (**a**) Attenuation coefficient; (**b**) phase velocity

12.5 Conclusions

The conclusions obtained from the present study are summarized as follows:

- The attenuation and dispersion properties for viscoelastic material over the wide range of frequencies were examined by the ultrasonic propagation experiments using the ultrasonic transducers having several characteristic frequencies.
- It was found that the viscoelastic properties on PMMA solid and hollow bars in the low frequency area could be evaluated by the first mode vibration using the 5-element model based on the three-dimensional exact theory.
- The higher-order mode vibration as well as the first mode vibration propagated on the hollow bar in the high frequency area.

References

1. Sackman, J.L., Kaya, I.: On the determination of very early-time viscoelastic properties. J. Mech. Phys. Solids **16**(2), 121–132 (1968)
2. Sogabe, Y., Tsuzuki, M.: Identification of the dynamic properties of linear viscoelastic materials by the wave propagation testing. Bull. JSME **29**(254), 2410–2417 (1986)
3. Sogabe, Y., Yokoyama, T., Yokoyama, T., Nakano, M., Kishida, K.: A split Hopkinson bar method for testing materials with low characteristic impedance. Dyn. Fract. **300**, 137–143 (1995)
4. Juea, Z., Shishengb, H., Lili, W.: An analysis of stress uniformity for viscoelastic materials during SHPB tests. Lat. Am. J Solids Struct **3**(2), 125–148 (2006)
5. Zhao, H., Gary, G.: A three dimensional analytical solution of the longitudinal wave propagation in an infinite linear viscoelastic cylindrical Bar. Application to experimental techniques. J. Mech. Phys. Solids **43**(8), 1335–1348 (1995)
6. Benatar, A., Rittel, D., Yarin, A.L.: Theoretical and experimental analysis of longitudinal wave propagation in cylindrical viscoelastic rods. J. Mech. Phys. Solids **51**(8), 1413–1431 (2003)
7. Flügge, W.: Viscoelasticity, p. 159. Springer, New York (1975)
8. Tamaogi, T., Sogabe, Y.: Attenuation and dispersion properties of longitudinal waves in PMMA Bar over a wide range of frequencies (in Japanese). J. JSEM **12**(3), 264–269 (2013)